On the Mechanisms of High-Temperature Intergranular Embrittlements of Ni_3Al-Zr Alloys

T.H. CHUANG and Y.C. PAN

Recent studies on the room-temperature fracture behavior of Ni_3Al-Zr alloys after preexposure at elevated temperatures show various types of intergranular failure. In the presently studied $Ni_{78}Al_{21}Zr_1B_{0.2}$ alloy, a strong intergranular fracture tendency at room temperature has been found after preexposure at 750 °C, which is caused by the grain boundary precipitation in this alloy. After short-term exposure above 1200 °C and bending fracture at room temperature, the alloy also suffers intergranular embrittlement due to grain boundary melting. The intergranular fracture appearance is quite different from that observed in a previous study for a $Ni_{77.4}Al_{22}Zr_{0.6}B_{0.2}$ alloy after air exposure for 100 hours at 1200 °C.[1] In that case, the intergranular fracture was accompanied by grain boundary diffusion (invasion) and segregation of oxygen. The mechanisms of these types of grain boundary failure are discussed.

I. INTRODUCTION

IT has been found that by adding trace amounts of boron to Ni_3Al, the problem of intergranular embrittlement can be drastically alleviated.[2] Thermal mechanical treatment can also increase the elongation of this alloy to about 40 pct.[3] By alloying with zirconium, Taniguchi *et al.* showed that the spallation of oxide film could be avoided by the interlocking of the oxide film to the Ni_3Al matrix through the growth of ZrO_2 along the grain boundaries of this alloy.[4] Mishima *et al.* found that zirconium increases the yield strength by solid solution strengthening.[5] Hsu *et al.*[6] and Lee *et al.*[7] showed that the creep rupture life of Ni_3Al increases with the zirconium additions. The influence of zirconium on grain boundary strengthening of Ni_3Al has never been reported, although it has long been employed as a beneficial element to prevent the formation of grain boundary precipitates in many superalloys.[8] Hsu *et al.*[6] indicated that the high-temperature intergranular embrittlement of Ni_3Al intermetallic compounds could not be alleviated by zirconium additions.

Intergranular embrittlement of intermetallic compounds after prior exposure to an oxygen-bearing atmosphere at elevated temperatures has been known since the 1960s and is commonly referred to as "grain boundary pest." Seybolt and Westbrook explained that this type of intergranular failure was caused by oxygen-induced grain boundary hardening due to oxygen segregation.[9] Another mechanism proposed by Turner *et al.* suggested that the intergranular failure in NiAl may be attributed to the repeated processes of oxygen penetration down the grain boundaries and oxidation of Al_2O to α-Al_2O_3 at the grain boundaries.[10] The internal strains produced by the volume expansion involved in the transformation would open up the material along the grain boundaries and allow oxygen to diffuse further into the interior in such a way as to continue the transformation.[11] However, α-Al_2O_3 precipitates on grain boundaries were not observed by Seybolt and Westbrook.[12] Turner *et al.*[10] also indicated that "grain boundary pest" only occurs at about 1400 °C. In our previous work, a ductile $Ni_{77.4}Al_{22}Zr_{0.6}B_{0.2}$ alloy was shown to suffer severe intergranular embrittlement after air exposure at 1200 °C for 100 hours.[1] The characteristics of this type of intergranular failure seem to be consistent with those of "grain boundary pest" during the 1960s.

Recently, intergranular failure after prior exposure above 1200 °C has also been found in a $Ni_{78}Al_{21}Zr_1B_{0.2}$ alloy, but the fracture appearance is quite different from the previously studied $Ni_{77.4}Al_{22}Zr_{0.6}B_{0.2}$ alloy. The grain boundary facets are very rough in this case. Also, an additional type of grain boundary failure has been shown in this alloy after preexposure at 750 °C. With this type of intergranular failure, many precipitates can be observed at grain boundaries. In this article, the two types of intergranular failure in $Ni_{78}Al_{21}Zr_1B_{0.2}$ alloy are reported, and the mechanisms of these types of intergranular failures for both Ni_3Al alloys with different zirconium contents are discussed.

II. EXPERIMENTAL PROCEDURE

The $Ni_{78}Al_{21}Zr_1B_{0.2}$ alloy in the present study was prepared by melting in a vacuum-induction furnace and casting into an iron mold to produce ingots 25 × 100 × 80 mm. The ingots were then cut and fabricated into 1.2-mm-thick sheets by repeated cold rolling (20 to 50 pct) and annealing (1150 °C/2 h and 1000 °C/1 h in air). The impurities included in this alloy were negligible. For example, the oxygen and carbon contents were less than 60 and 70 ppm respectively, the hydrogen content was less than 10 ppm, and the sulfur content was less than 20 ppm by weight.

The sheet materials were then sliced into specimens having an area 20 × 10 mm. All of these specimens were polished through 1200 grit and further annealed at various temperatures, mostly in an air furnace. To compare the effect of oxygen, some specimens were annealed in a vacuum furnace under a vacuum of 10^{-4} Pa.

T.H. CHUANG, Professor, is with the Institute of Materials Science and Engineering, National Taiwan University, Taipei, Taiwan, Republic of China. Y.C. PAN, formerly Doctoral Candidate, Institute of Materials Science and Engineering, National Taiwan University, is Associate Scientist, Chung-Shan Institute of Science and Technology, Taoyuan, Taiwan, Republic of China.

Manuscript submitted January 30, 1991.

The prior exposed materials as well as the as-thermomechanically treated materials, were then notched and fractured by impact bending at ambient temperature in air with a hammer. The fracture surfaces were observed by scanning electron microscopy (SEM) and analyzed with energy-dispersive X-ray spectroscopy (EDS).

Some specimens were cut into small slices 16 × 3 × 1 mm and also notched at the middle of the two long edges for Auger analysis. For this purpose, a Physical Electronics Industries Model 600 Scanning Auger System was used. In this case, specimens were fractured *in situ* by impact bending with a hammer at a system pressure of 10^{-9} Pa.

Differential thermal analyses (DTA) were also performed with the heating rate of 10 °C/min under nitrogen atmosphere.

III. EXPERIMENTAL RESULTS

Previous study[1] by the authors has shown that an originally ductile $Ni_{77.4}Al_{22}Zr_{0.6}B_{0.2}$ alloy exhibited completely intergranular fracture after air exposure at 1200 °C for 100 hours. The grain boundary facets are very smooth, with some oxide particles on them. Auger analyses indicated that a very large amount of oxygen segregated within several monolayers at these grain boundaries.

In the present study, an as-thermomechanically treated $Ni_{78}Al_{21}Zr_1B_{0.2}$ alloy also shows originally an obviously ductile fracture mode at room temperature (Figure 1). After air exposure at 560 °C for 492 hours and at 900 °C and 1050 °C for 96 hours, the material remains ductile. However, preexposure at 750 °C in air results in a drastically increasing tendency toward intergranular fracture, as shown in Figure 2. The grain boundary facets are smooth for shorter exposure times. But, with increasing time, the fraction of intergranular failure increases, and the grain boundary facets become more cavernous. The intergranular embrittlement of this alloy at 750 °C cannot be avoided by changing the atmosphere from air to 10^{-4} Pa vacuum. Metallography shows that many precipitates exist along the grain boundaries and in the grains of this alloy after preexposure at this temperature (Figure 3). Accompanying the precipitates, many grain

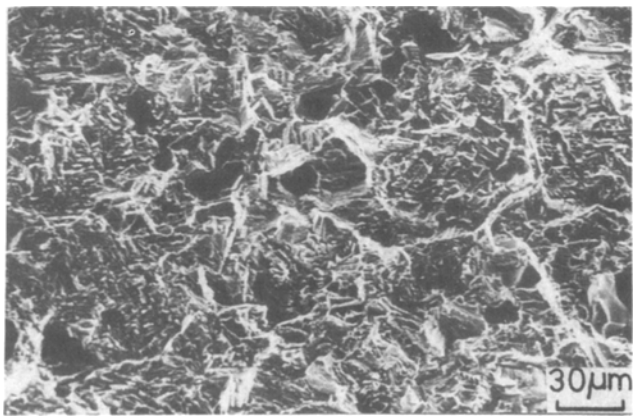

Fig. 1—The fracture surface of the as-thermomechanically treated $Ni_{78}Al_{21}Zr_1B_{0.2}$ alloy (SEM).

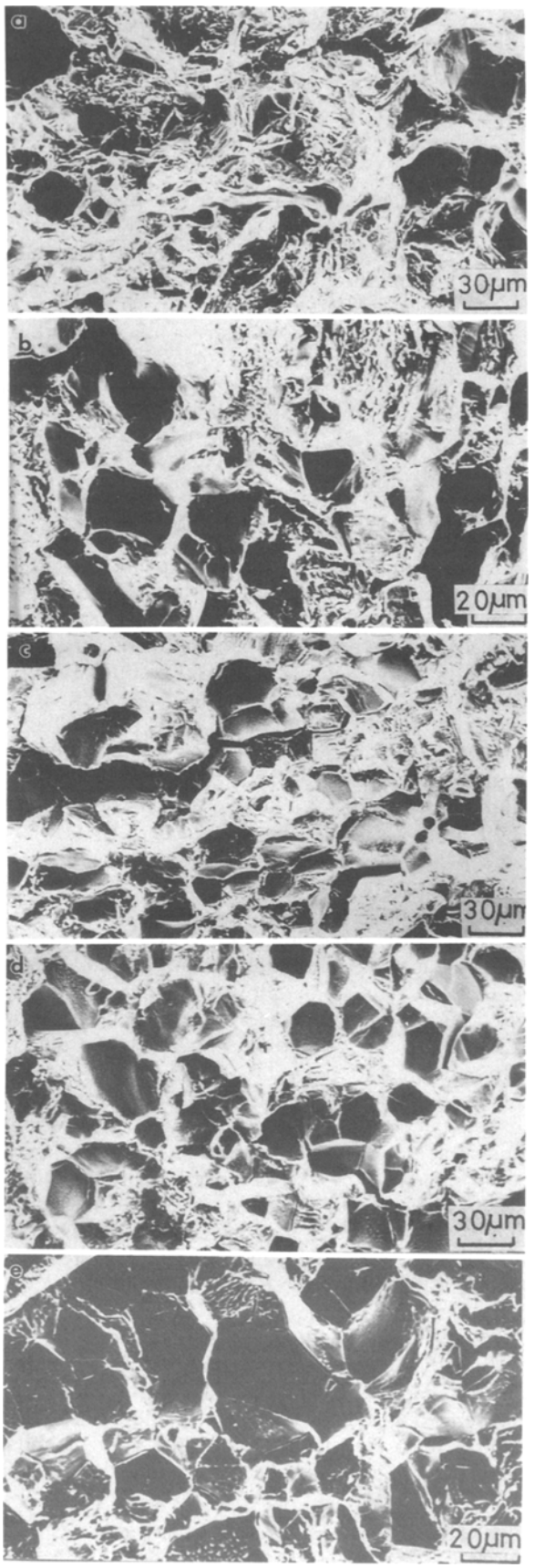

Fig. 2—Intergranular fracture of the $Ni_{78}Al_{21}Zr_1B_{0.2}$ alloy after air exposure at 750 °C for (*a*) 2 h, (*b*) 24 h, (*c*) 96 h, (*d*) 240 h, and (*e*) 672 h (SEM).

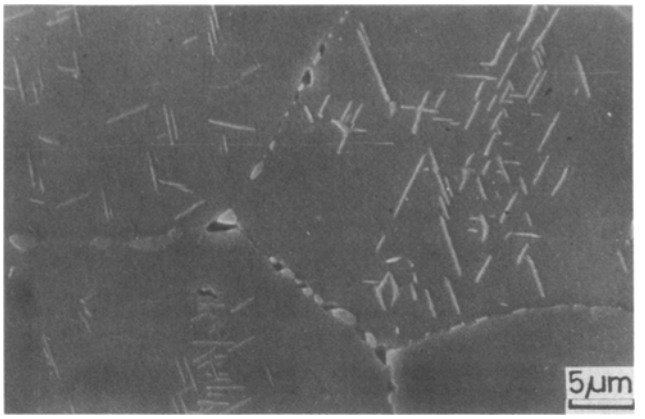

Fig. 3—Microstructure of the precipitated particles formed in the $Ni_{78}Al_{21}Zr_1B_{0.2}$ alloy after air exposure at 750 °C for 500 h.

boundary cavities can also be observed in Figure 3. Further studies show that the precipitates also exist at 700 °C and 800 °C. However, the formation and growth of these precipitates are much slower than those at 750 °C. This phenomenon of grain boundary precipitates disappears below 700 °C and above 800 °C, ever after long-term exposure.

After air exposure at 1200 °C for 96 hours, the grain boundaries of the specimens are completely oxidized, and the material shows severe intergranular embrittlement (Figure 4). However, after prior exposure at this temperature for shorter times, such as 17 hours, the interiors of the specimens still remain partially ductile, in spite of the severely oxidized layer formed on the surface.

Raising the prior exposure temperature above 1200 °C for only 80 minutes results in an increasing tendency toward intergranular fracture. At 1300 °C, the fracture is completely intergranular (Figure 5(e)). This embrittlement occurs after prior exposure not only to an atmosphere but also to 10^{-4} Pa vacuum. As seen in Figure 5, above 1280 °C the grain boundary facets become rough and are quite different from those observed in the $Ni_{77.4}Al_{22}Zr_{0.6}B_{0.2}$ alloy after air exposure at 1200 °C for 100 hours. In fact, such intergranular fracture with rough grain boundary facets was not observed

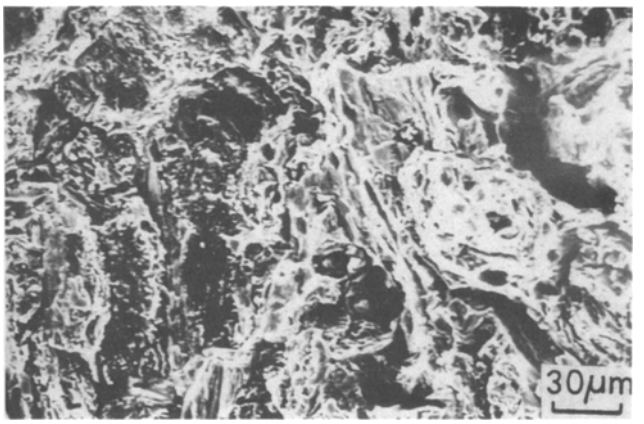

Fig. 4—The fracture surface of the $Ni_{78}Al_{21}Zr_1B_{0.2}$ alloy after air exposure at 1200 °C for 96 h.

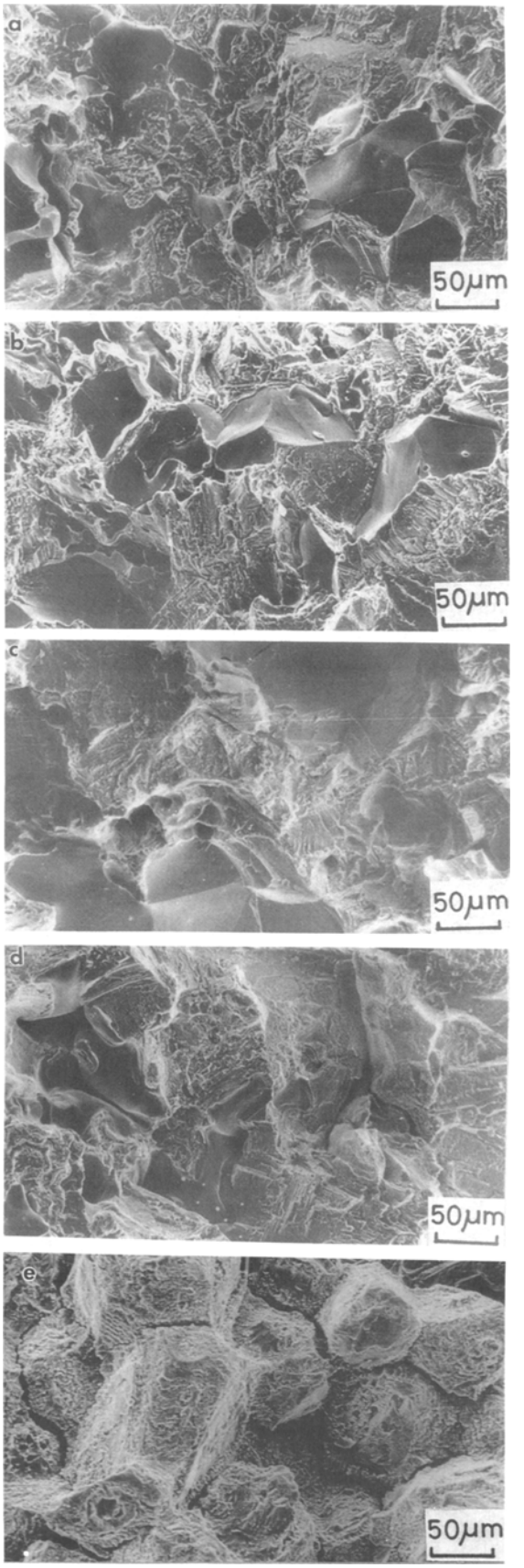

Fig. 5—Fracture surface of the $Ni_{78}Al_{21}Zr_1B_{0.2}$ alloy after prior exposure at (*a*) 1200 °C, (*b*) 1220 °C, (*c*) 1250 °C, (*d*) 1280 °C, and (*e*) 1300 °C for 80 min (SEM).

in that alloy, even after the prior exposure at 1300 °C in air and in vacuum. The intergranular fracture observed in $Ni_{78}Al_{21}Zr_1B_{0.2}$ alloy after prior exposure at temperatures from 1200 °C to 1280 °C shows predominantly smooth grain boundary facets. However, a small area with rough appearance can be found on local sites of some grain boundary facets. It seems that the proportion of rough area to smooth area on the grain boundary facets in the intergranular fracture regions also increases with the increase of preexposure temperature from 1200 °C to 1300 °C.

Some specimens of this $Ni_{78}Al_{21}Zr_1B_{0.2}$ alloy after air exposure at 1300 °C for 2 hours have been analyzed with Auger electron spectroscopy (AES). The results indicate that the nickel and aluminum contents on the intergranular fractured facets are strongly inhomogeneous, both with the average deviations of about 8 at. pct. Also, the oxygen and carbon contents are enriched at the grain boundaries of these AES specimens. The fracture surfaces have also been analyzed by EDS in the scanning electron microscope. The results in Figure 6 indicate that a large amount of zirconium exists on the intergranular fracture facets.

To clarify the mechanism of this type of grain boundary failure, a metallographic analysis was conducted and the results are shown in Figures 7(a) through (e) for specimens after prior exposure at 1200 °C, 1220 °C, 1250 °C, 1280 °C, and 1300 °C for 80 minutes, respectively. These microstructures correspond to the fractographs in Figures 5(a) through (e). These micrographs indicate that grain boundary melting occurred at the triple points of the grain boundaries in the interior of this alloy after prior exposure at these temperatures. The number of locations at which grain boundary melting occurred increases with an increase of exposure temperature. The high-magnification scanning electron micrograph in Figure 8 shows that the regions with grain boundary melting at triple points possess a lamellar structure, which could result from an eutectic reaction in these regions. The EDS analyses in Figure 9 show that these regions

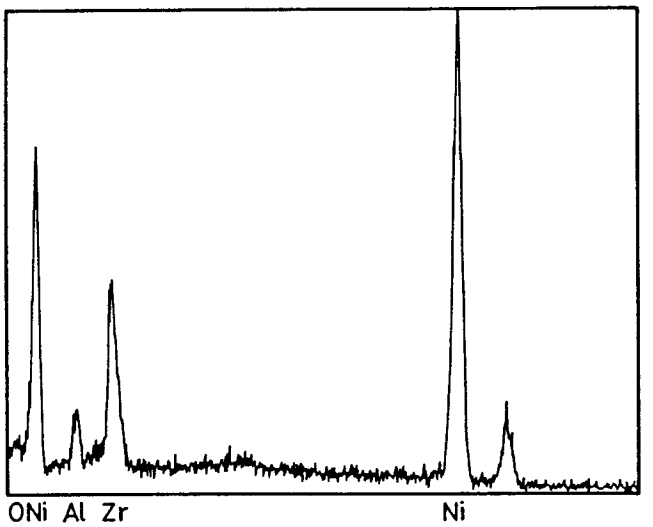

Fig. 6—EDS analysis of the fracture surface of $Ni_{78}Al_{21}Zr_1B_{0.2}$ alloy after prior exposure at 1300 °C for 2 h.

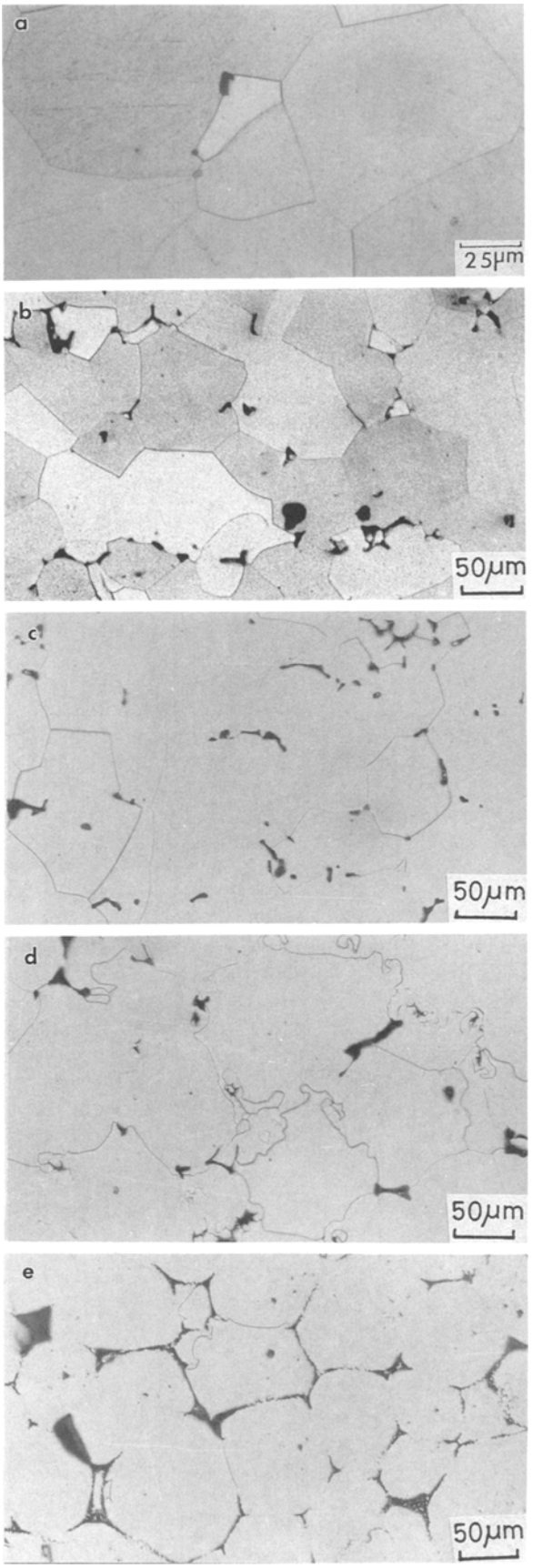

Fig. 7—Microstructure of the $Ni_{78}Al_{21}Zr_1B_{0.2}$ alloy after prior exposure at (*a*) 1200 °C, (*b*) 1220 °C, (*c*) 1250 °C, (*d*) 1280 °C, and (*e*) 1300 °C for 80 min optical microscopy.

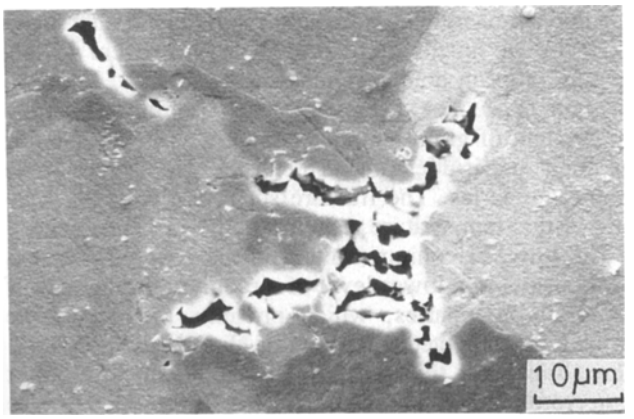

Fig. 8—High-magnification view of the grain boundary melting region at the triple point of grain boundaries shown in Fig. 6(e) (SEM).

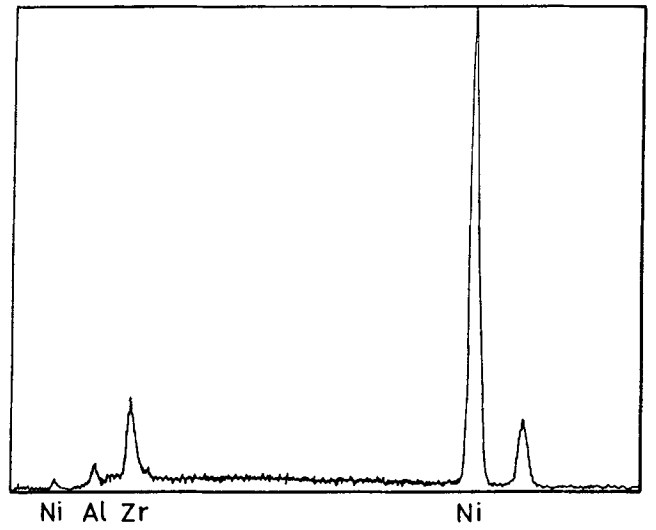

(*a*)

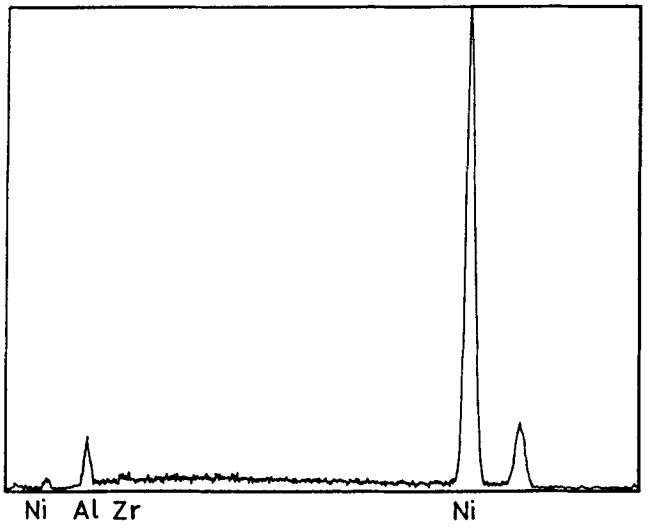

(*b*)

Fig. 9—EDS spectra taken from (*a*) the triple point and (*b*) the interior of grain for the $Ni_{78}Al_{21}Zr_1B_{0.2}$ alloy after prior exposure at 1300 °C for 80 min.

are rich in zirconium, while only a little zirconium can be detected in the grain.

Differential thermal analyses show that there exists an endothermic transition point at about 1190 °C for the $Ni_{78}Al_{21}Zr_1B_{0.2}$ alloy (Figure 10(a)). For comparison, the DTA result for the $Ni_{77.4}Al_{22}Zr_{0.6}B_{0.2}$ alloy is shown in Figure 10(b). For this analysis, a transition peak near 1190 °C cannot be found.

IV. DISCUSSION ON THE MECHANISMS

As the result of additions of 0.2 at. pct B and thermomechanical treatments, both the $Ni_{77.4}Al_{22}Zr_{0.6}B_{0.2}$ and $Ni_{78}Al_{21}Zr_1B_{0.2}$ alloys exhibited excellent ductility. However, the $Ni_{77.4}Al_{22}Zr_{0.6}B_{0.2}$ alloy suffered severe intergranular embrittlement after a long-term air exposure at 1200 °C for 100 hours. Auger analysis indicated that the grain boundary failure in this case is attributed to the grain boundary segregation of oxygen. A mechanism was proposed in which the protective oxide film on the surface of this alloy was thought to be disrupted at this high temperature. This allowed the oxygen from the air atmosphere to diffuse into and along the grain boundaries

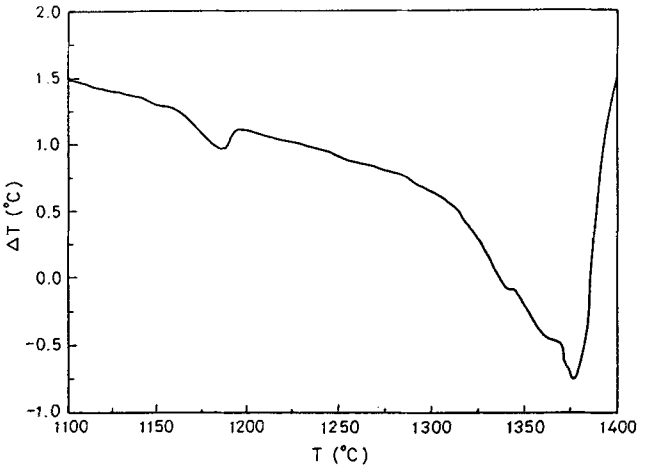

(*a*)

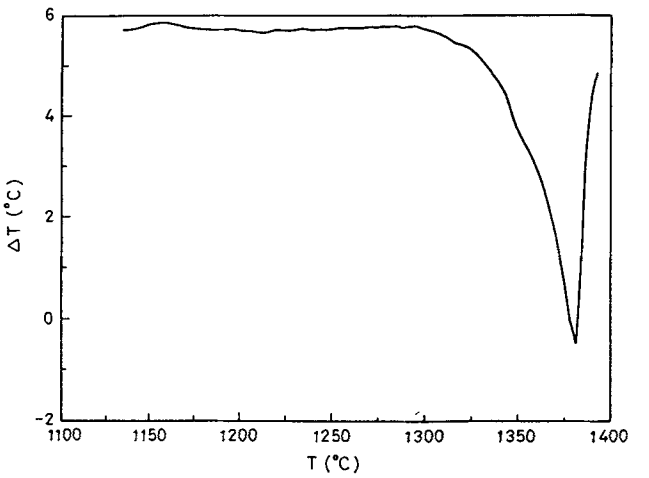

(*b*)

Fig. 10—DTA curves for (*a*) $Ni_{78}Al_{21}Zr_1B_{0.2}$ and (*b*) $Ni_{77.4}Al_{22}Zr_{0.6}B_{0.2}$.

and to segregate on them. The segregation of oxygen on the grain boundaries was then thought to cause the loss of grain boundary cohesion and result in the intergranular embrittlement in the alloy.

In the present $Ni_{78}Al_{21}Zr_1B_{0.2}$ alloy, a drastically increased tendency toward intergranular fracture has been found after prior exposure at 750 °C in an air atmosphere and in 10^{-4} Pa vacuum. The grain boundary failure in this case may be related to the precipitation reaction mostly occurring at this temperature (Figure 3). The different thermal expansion coefficients of the precipitate phase and the matrix cause many cavities to form on the grain boundaries. It is proposed that the grain boundary hardening caused by the precipitate particles and the associated formation of grain boundary cavities result in the decohesion and embrittlement of the grain boundary. As the exposure time increases, the precipitates grow and more cavities form. As such, the tendency toward intergranular fracture also increases. In the $Ni_{77.4}Al_{22}Zr_{0.6}B_{0.2}$ alloy, the zirconium content is lower than its equilibrium solubility. As such, the formation of a precipitate phase at 750 °C is avoided. Therefore, the intergranular embrittlement observed in $Ni_{78}Al_{21}Zr_1B_{0.2}$ at this temperature is not observed in the $Ni_{77.4}Al_{22}Zr_{0.6}B_{0.2}$ alloy.

After prior exposure at 1200 °C in an air furnace, it has been shown that the oxidized scale formed on the $Ni_{78}Al_{21}Zr_1B_{0.2}$ alloy is thicker than that on the $Ni_{77.4}Al_{22}Zr_{0.6}B_{0.2}$ alloy. This result indicates that the oxidation rate of the former alloy with the higher zirconium content is greater. The greater consumption of the oxygen on the external surface of the Zr-rich alloy prevents the deep penetration of oxygen along the grain boundaries into the interior of the material. Therefore, the intergranular embrittlement occurring in the $Ni_{77.4}Al_{22}Zr_{0.6}B_{0.2}$ alloy and thought to be caused by the grain boundary segregation of oxygen after air exposure at 1200 °C does not appear in the $Ni_{78}Al_{21}Zr_1B_{0.2}$ alloy.

Another example of severe intergranular embrittlement has been found in the $Ni_{78}Al_{21}Zr_1B_{0.2}$ alloy after short-time prior exposure in air and even in 10^{-4} Pa vacuum at temperatures above 1200 °C. Metallographic observations (Figure 8) show that grain boundary melting had occurred, as evidenced by the lamellar structure at the triple points of grain boundaries. In conjunction with EDS analyses, these metallographic observations indicate that this melting could be caused by the localized eutectic reaction of Ni_5Zr and Ni at the grain boundaries. With reference to the Ni-Zr phase diagram,[13] an eutectic point of Ni_5Zr and Ni actually exists at 1172 °C. Since the enrichment of grain boundaries of Ni_3Al intermetallic compounds by zirconium has been proposed by many workers,[3,14–16] the occurrence of this localized eutectic reaction at the grain boundaries seems to be quite reasonable. Also, the DTA peak at about 1190 °C (Figure 10(a)) confirms this inference. Because grain boundaries occupy only a small volume fraction of the polycrystalline material, the DTA peak for this localized reaction is much smaller than the peak at 1350 °C for the melting of the grains themselves. The slightly higher temperature obtained on the DTA curve for melting of the eutectic may be attributed to the deviation of the chemical composition for the eutectic reaction in the quaternary alloy from that in the binary Ni-Zr system.

Although intergranular fracture can be found only above 1220 °C, the metallographic observations reveal a slight amount of grain boundary melting at 1200 °C, as shown in Figure 7(a). The discrepancy may simply result from the amount of grain boundary melting at 1200 °C being so small that it does not result in the decohesion at the grain boundaries. The fracture surface after prior exposure at this temperature remain ductile in appearance.

The lower zirconium content in the $Ni_{77.4}Al_{22}Zr_{0.6}B_{0.2}$ alloy results in a lower level of zirconium enrichment of the grain boundaries, which prevents the occurrence of the localized eutectic reaction of Ni_5Zr and Ni on them. The absence of this type of grain boundary failure at temperatures from 1200 °C to 1300 °C in the $Ni_{77.4}Al_{22}Zr_{0.6}B_{0.2}$ alloy could, therefore, be understood on this basis.

V. CONCLUSIONS

As shown in a previous work,[1] a $Ni_{77.4}Al_{22}Zr_{0.6}B_{0.2}$ alloy suffers severe intergranular embrittlement after prior air exposure at 1200 °C for 100 hours. The grain boundary facets are very smooth, with some oxide particles on them. This intergranular failure is attributed to the breakdown of the protective oxide film and the invasion and segregation of oxygen on the grain boundaries.

In the present study, a $Ni_{78}Al_{21}Zr_1B_{0.2}$ alloy also suffers intergranular embrittlement after short-time prior exposure above 1200 °C in air and 10^{-4} Pa vacuum. At 1300 °C, a completely intergranular fracture has been found. However, the grain boundary facets are rough. This type of grain boundary failure is associated with grain boundary melting above 1200 °C, which is caused by the eutectic reaction of Ni_5Zr and Ni on the grain boundaries.

In addition to the grain boundary melting above 1200 °C, another type of grain boundary failure has been found in the present $Ni_{78}Al_{21}Zr_1B_{0.2}$ alloy after preexposure at 750 °C in air and in 10^{-4} Pa vacuum. This is attributed to the grain boundary precipitates formed at this temperature. The tendency toward intergranular embrittlement increases with increasing exposure time. This is consistent with the growth of these precipitated particles on grain boundaries.

REFERENCES

1. T.H. Chuang, Y.C. Pan, and S.E. Hsu: *Metall. Trans. A*, 1991, vol. 22A, pp. 1801-09.
2. K. Aoki and O. Izumi: *J. Jpn. Inst. Met.*, 1979, vol. 43, pp. 1190-96.
3. C.T. Liu, C.L. White, and J.A. Horton: *Acta Metall.*, 1985, vol. 33, pp. 213-29.
4. S. Taniguchi, T. Shibata, and H. Tsuruoka: *Oxid. Met.*, 1986, vol. 26, pp. 1-18.
5. Y. Mishima, S. Ochiai, N. Hanao, M. Yodogawa, and T. Suzuki: *Trans. Jpn. Inst. Met.*, 1986, vol. 27, pp. 656-64.
6. S.E. Hsu, N.N. Hsu, C.H. Tong, P.H. Hu, and J.Y. Ma: *Proc. of the 1986 Annual Conf. of the Chinese Society for Materials Science*, June 21–22, 1986, Taichung, Taiwan, 1986, pp. 423-29.
7. S.Y. Lee, S.J. Liu, C.H. Tong, and S.E. Hsu: *Proc. of the 1987 Annual Conf. of the Chinese Society for Materials Science*, May 23–24, 1987, Hsinchu, Taiwan, pp. 303-07.
8. W. Dienst: in *Hoch-Temperatur-Werkstoffe*, Werkstofftechnische Verlag, Karlsruhe, Germany, 1978, p. 115.
9. A.U. Seybolt and J.H. Westbrook: *Acta Metall.*, 1964, vol. 12, pp. 449-58..

10. P.A. Turner, R.T. Pascoe, and C.W.A. Newey: *J. Mater. Sci.*, 1966, vol. 1, pp. 113-15.
11. P.A. Turner, R.T. Pascoe, and C.W.A. Newey: *J. Mater. Sci.*, 1967, vol. 2, p. 197.
12. A.U. Seybolt and J.H. Westbrook: *J. Mater. Sci.*, 1967, vol. 2, pp. 196-97.
13. *Binary Alloy Phase Diagram*, T.B. Massalski, J.L. Murray, L.H. Bennett, and H. Baker, eds., ASM, Metals Park, OH, 1986, p. 1779.
14. J.D. Kuenzly and D.L. Douglass: *Oxid. Met.*, 1974, vol. 8, pp. 139-78.
15. R.F. Decker and C.T. Sims: in *The Superalloys*, C.T. Sims and W.C. Hagel, eds., John Wiley and Sons Inc., New York, NY, 1972, p. 33.
16. T.H. Chuang: *Mater. Sci. Eng.*, 1991, vol. A141, pp. 169-78.